Utah FORGE– 2025 Annual R&D Workshop

9-3664 - Development and Testing of Tagged Proppant for Fracture Conductivity Enhancement and Reservoir Characterization in EGS

- PI: Ahmad Ghassemi
- Organization: The University of Oklahoma
- Presenters: Ahmad Ghassemi (OU)
- Subcontractor: Guoqiang Li (LSU); Shahrzad Roshnakhah (U of Utah)

- April 1 (June 1), 2024 to September 30, 2026

Objectives and Purpose

- Test and develop new proppants that can be used in geothermal conditions of at least of 250 ˚C and differential pressures of 35-70 MPa

- Characterize the materials and carry out conductivity tests under HTHP

- Test a few proppant materials e.g., garnet, petcoke, and polymer. The polymer material will be used to generate sub-100 mesh light and high strength proppant. This proppant will also be doped with conductive agents having electromagnetic sensitivity for potential diagnostics

- **Significance& Impact**: Designing and testing of next generation proppants and interrogating their performance in HTHP condition of interest to EGS would provide the means for sustaining hydraulic fracture conductivity, and enabling effective heat production from EGS concepts relying on multi-stage fracturing

Methods/Approach

- Conduct proppant crush tests on heated proppants. Procure proppant materials and consider modifications if necessary and determine their index properties. Examine the durability of selected proppant materials in the presence of geothermal fluids at high temperatures.
- Conduct conductivity tests at high temperature and pressure using standard and new test geometries. Determine long-term hydraulic conductivity of the uncoated/untagged proppant materials at various stress and temperature conditions.
- Develop new polymer materials that can sustain high temperatures and pressure.
- Conduct simulation modeling to study controls on proppant resistance. Modeling the effect of particle size, size distribution, shape, and type on crush resistance and deformational as well as hydraulic (permeability evolution) of particulate packs to inform lab developments and field implementations.
- Examine the hydraulic conductivity, and electrical detectability of the coated/tagged proppant materials in large fracture(s) created in granite blocks.
- Conduct modeling on proppant transport and deposition in fracture networks

Methods/Approach

- Procure proppant materials and consider modifications if necessary and determine their index properties. Examine the durability of selected proppant materials in the presence of geothermal fluids at high temperatures (M1-M6)

- Design, synthesis, and characterization of polymeric proppant (M1-M9)
  - Shape memory polymer (SMP) is a new member of the smart materials family. Unlike conventional thermoset polymers, thermoset SMPs, when deformed into permanent deformation, either in glassy state, or in glass transition zone, or in rubbery state, can recover to their original shape under proper stimuli (e.g., heat, light, and moisture).

- Determine crush resistance (K-value) and crush strength for both dry and wet-heated samples for the uncoated/untagged proppant materials (ISO 13503-2); study failure mechanisms and modes using modeling and comparison with test results (M3-M12).

- Determine long-term hydraulic conductivity of the uncoated/untagged proppant materials at various stress and temperature conditions (M6-M12).

Methods/Approach

- Task 8.0: Examine the hydraulic conductivity, and electrical detectability of the coated/tagged proppant materials in large fracture(s) created in granite blocks. (M24-30)

- Quantify/map the cyclic stress- and temperature-dependent hydro-thermo-mechanical behavior of selected materials under HTHP conditions. Simulate proppant transport, placement and proppant bed formation using different proppants and fluid with temperature dependent viscosity (M24-30).

	Budget Year	Year 1			
	Actual Qtr.	Q2 24	Q3 24	Q4 24	Q1 25
	Project Qtr.	Q1	Q2	Q3	Q4
Project Milestones	Deliverable				
Task 0 – Project Management and Planning			•		
Task 1 – Procure proppant materials and consider modifications if necessary and determine their index properties. Examine the durability of selected proppant materials in the presence of geothermal fluids at high temperatures					
Milestone 1.1 -Review the selected proppant materials and determine their index properties.					x
Milestone 1.2 -Characterize the resistance of selected proppant materials to geothermal fluids and high temperatures.					x
Task 2 – Design, synthesis, and characterization of polymeric proppant					x
Milestone 2.1-A new high temperature thermoset is designed, synthesized, and tested.					
Milestone 3.3 -Complete the determination of crush strength of the uncoated/untagged proppant materials through the modified triaxial crush testing. Simulations of controls on proppant and pack strength completed					x
Task 4 – Determination of crush resistance (K-value) and crush strength for both dry and wet-heated samples for the uncoated/untagged proppant materials; study failure mechanisms and modes using modeling and comparison with test results					
Milestone 4.1 -Completion of long-term hydraulic conductivity under HTHP conditions for the uncoated/untagged proppants, and correlation of conductivity, closure stress, and temperature. index properties.					
Go/No-Go Decision Point #1: Selected and manufactured proppants characterized, crush tests and long-term conductivity tests completed (at least 2 tests per proppant type) under pressure and temperature conditions of 35-70 MPa, and up to 250C.					

Technical Accomplishments and Progress

Proppant Type	Sizes	Bulk Density (gm/cc)	Proppant shape (X=Roundness, Y=Sphericity	Packing strength (psi)	K-value	Fine generates at K-value (%)
PC	10_35	1.09	(0.7, 0.7)	2100	2K	6.67
	35_60	0.99	(0.3, 0.5)	1800	2K	8.90
LDC	10_35	1.21	(0.9, 0.9)	3600	4K	7.77
	35_60	1.27	(0.9, 0.9)	5700	7K	9.70
RC	10_35	1.60	(0.9, 0.9)	10200	15K	7.50
	35_60	1.53	(0.9, 0.9)	12100	17K	9.03

Sample ID	Proppant type	Proppant bed shape	Proppant bed thickness (mm)	Proppant bed weight (g)	Host rock dimension (mm)	
					Top section	Bottom section
Sample A	LDC (10_35)	circular	5.00	22.00	30.50	30.80
Sample ReA	LDC (10_35)	rectangular	4.00	35.00	30.30	28.50
Sample B	RC (10_35)	circular	5.00	25.40	30.80	29.00
Sample ReB	RC (10_35)	rectangular	3.30	39.00	30.30	28.50
Sample C	PC (10_35)	circular	5.00	35.50	26.50	33.00

Technical Accomplishments and Progr

Sample Rec Length: 7.1 inch Width: 1.6 inch	Proppant type	Proppant thickness :1 lb/ft²	Host Sample Height (inches)
Sample A	Low Density Ceramic (LDC)	4 mm (36 gr)	Top part: 1.2 Bot part: 1.1
Sample B	Resin Coated	3.1 mm (36 gr)	Top part: 1.2 Bot part: 1.1
Sample C	Petroleum Coke	4.5 mm (36gr)	Top part: 1.2 Bot part: 1.4

Sample (Circle) 2.69 inch diameter	Proppant type	Proppant thickness	Host Sample Height: (inches)
Sample A	Low Density Ceramic (LDC)	5 mm (1.2 lb/ft², 22 gr)	Top disc: 1.2 Bot disc: 1.2
Sample B	Resin Coated	5 mm (1.4 lb/ft², 25 gr)	Top disc: 1.2 Bot disc: 1.1
Sample C	Petroleum Coke	9 mm (2 lb/ft², 35 gr)	Top disc: 1 Bot disc: 1.3

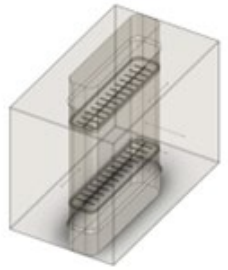

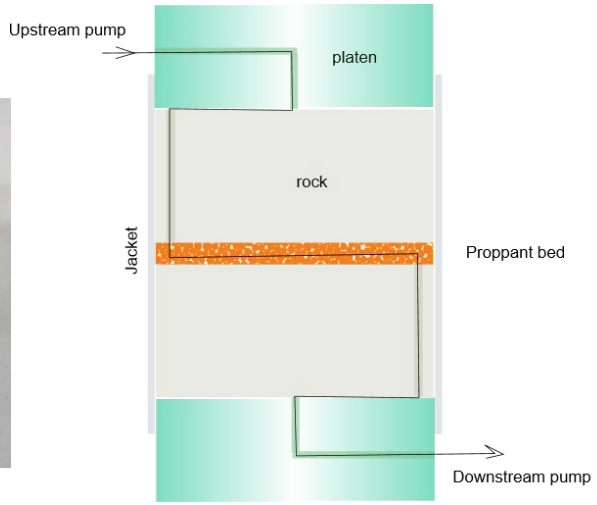

Sample A (LDC proppant)

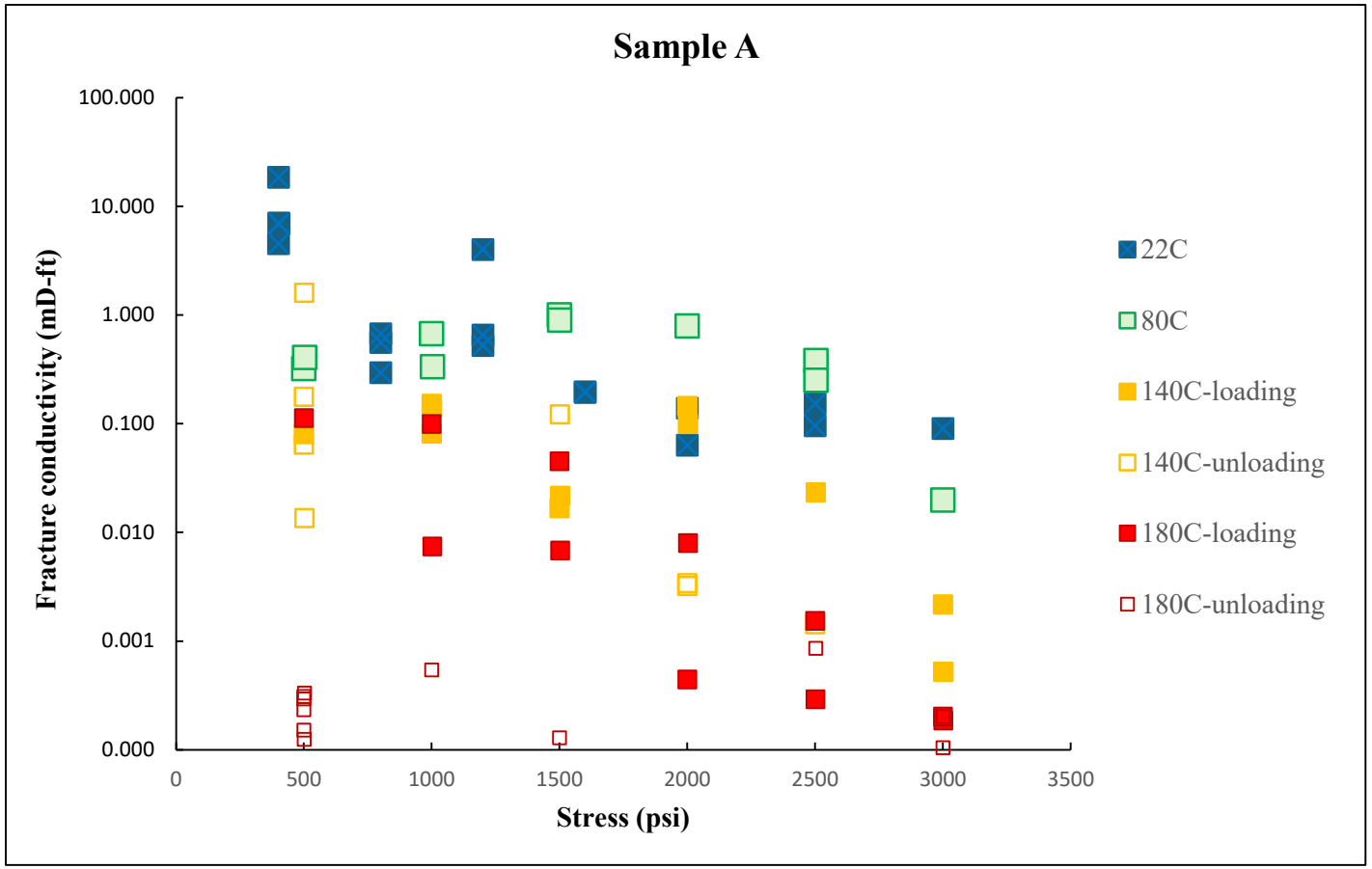

Overall, fracture conductivity decreases with both increasing temperature and applied stress (cold-colored spots of low temperatures overlying the hot-colored). While data shows some scattering - indicative of unstable flow behavior characteristic of proppant packs (unlike consolidated rock formations) - the decreasing trend remains statistically evident. Notably, permeability reduction at elevated temperatures appears irreversible, persisting even during stress unloading cycles (180C - unloading).

Overflow samples following thermal treatment at 80°C, 140°C, 180°C, and 220°C (left to right). The progressive darkening of solution color indicates increasing dissolution of material components at elevated temperatures.

Sample ReA (LDC proppant)

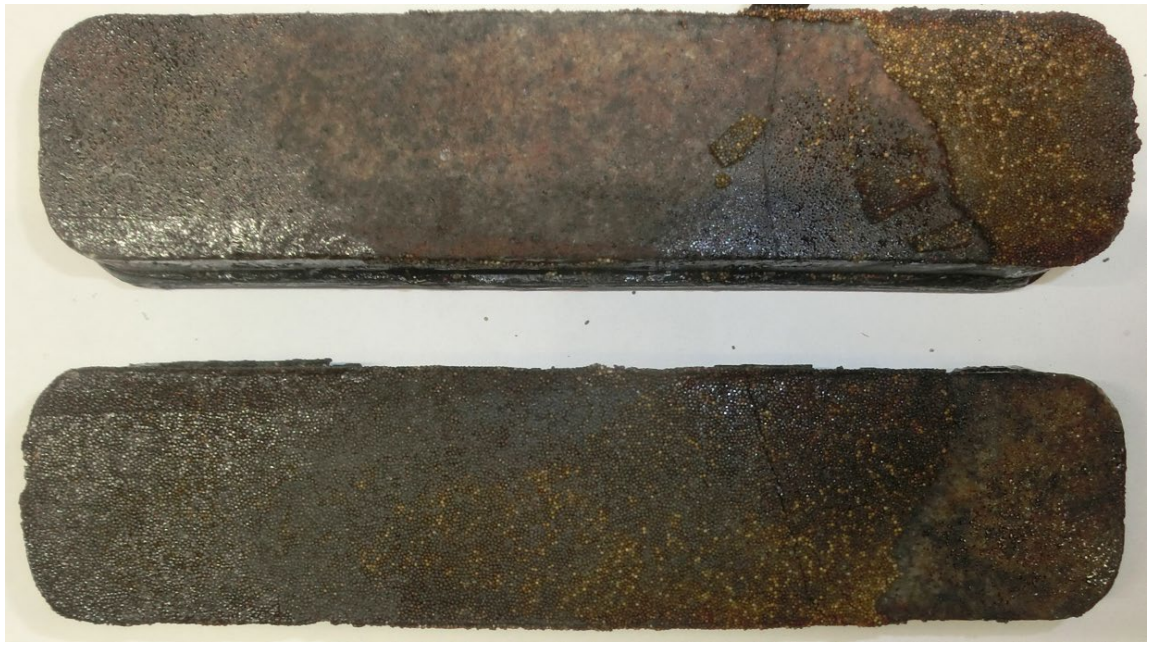

Proppant bed after exposure to high temperature and pressure. The bed remains largely intact, indicating strong structural stability under simulated downhole conditions.

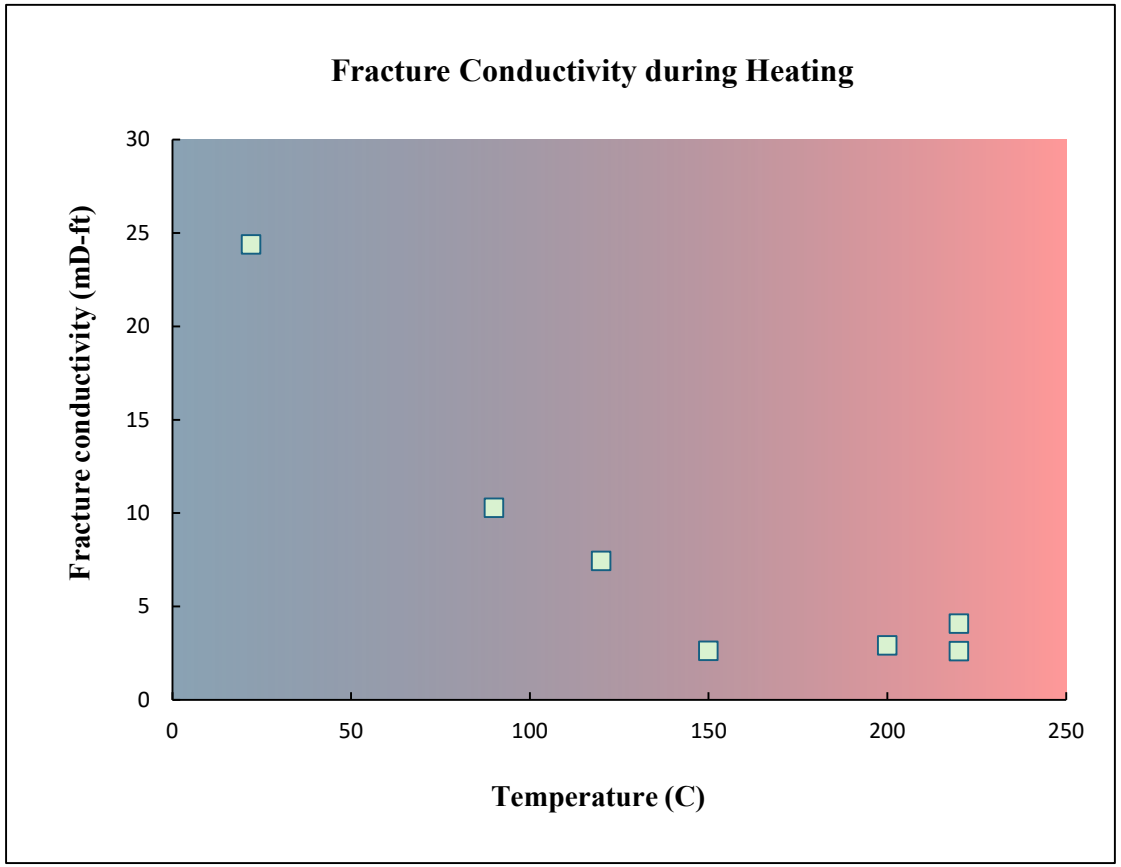

Fracture conductivity response during heating under constant axial stress (1000 psi) and a fixed pressure differential (3 psi) between upstream and downstream pumps. A general decrease in conductivity is observed as temperature increases.

Sample ReA (LDC proppant)

Proppant bed after exposure to high temperature and pressure. The bed remains largely intact, indicating strong structural stability under simulated downhole conditions.

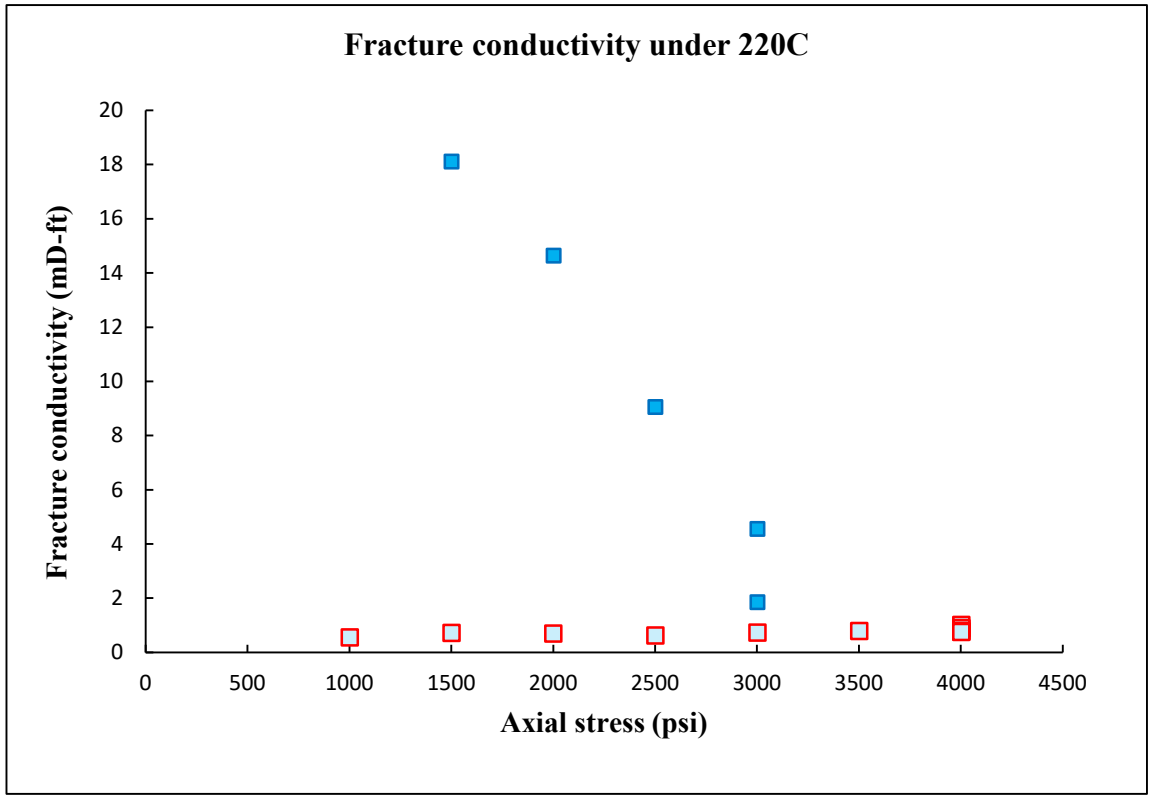

Under constant temperature conditions, fracture conductivity tends to decrease with increasing axial stress. However, once reduced, conductivity may not fully recover even after the axial stress is lowered, suggesting possible irreversible deformation or proppant rearrangement.

Sample ReA (LDC proppant)

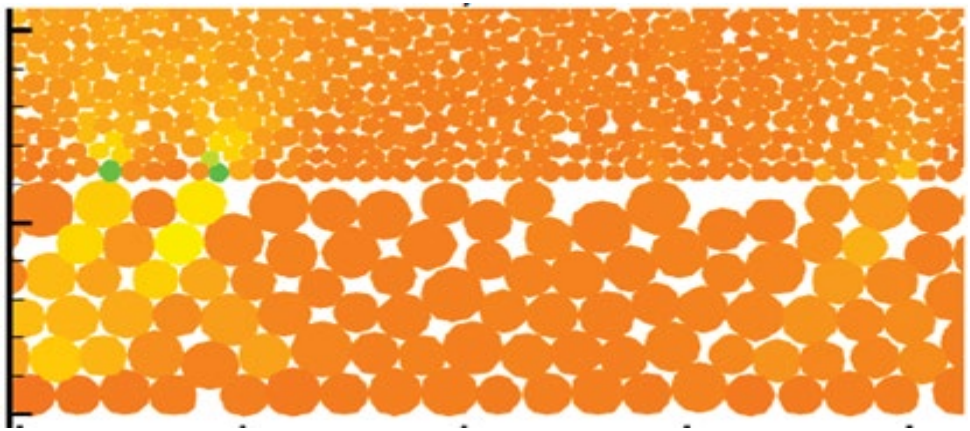

- The stress distribution within the proppant bed is highly heterogeneous, as supported by numerical modeling (Mattson et al., 2014).
- **In the figure above, bright-colored particles highlight areas of stress concentration**.
- Post-test observations of fractures on the rock surface (figure on the right) further confirm this speculation, suggesting localized stress concentrations during test.

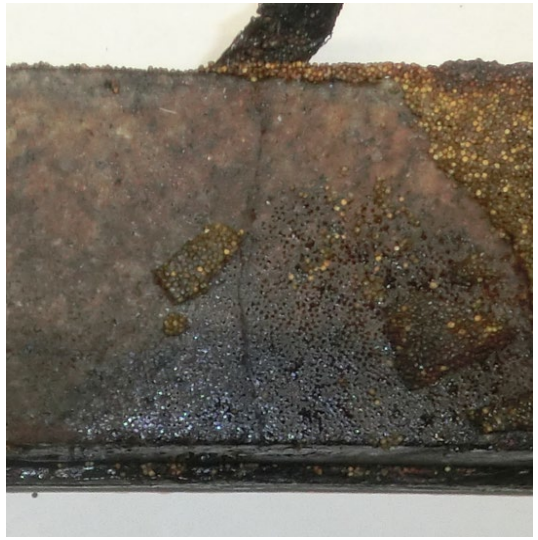

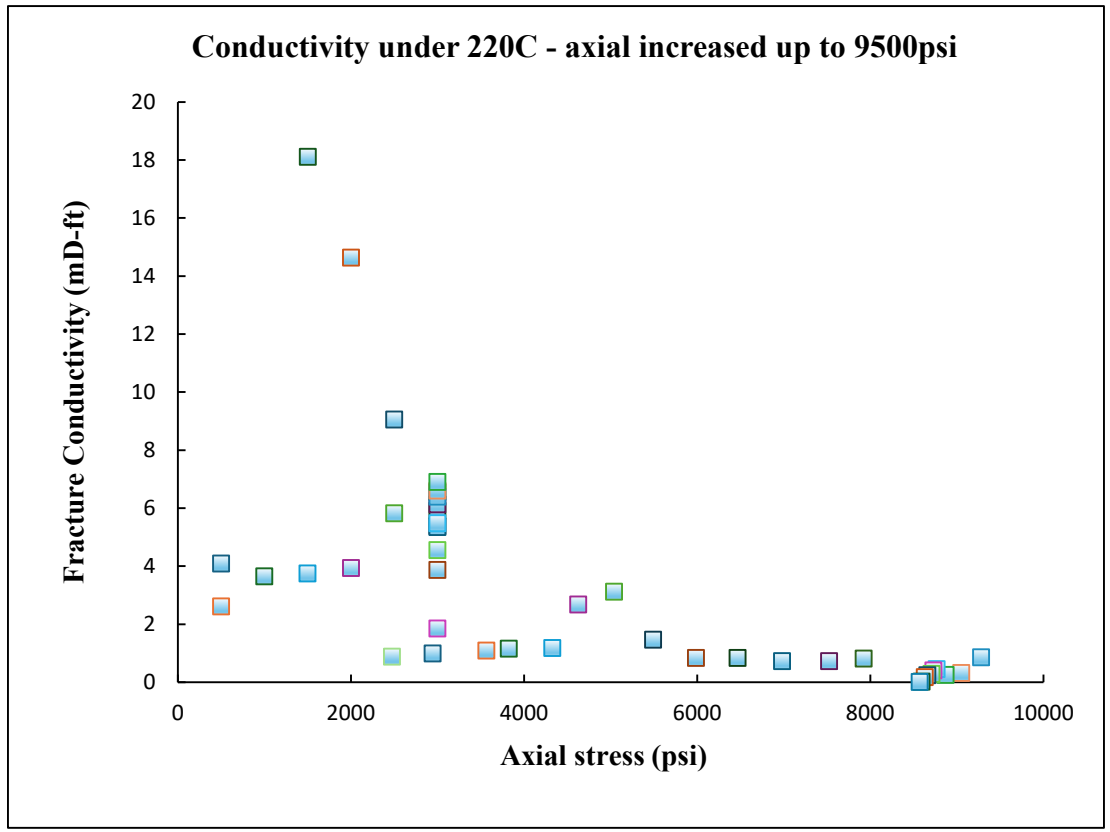

The correlation between stress and conductivity is complex due to the highly heterogeneous stress distribution within the proppant bed, which can be altered by fluid flow. Permeability varies with loading history but generally decreases as stress increases from a statistical standpoint.

Sample B (RC proppant)

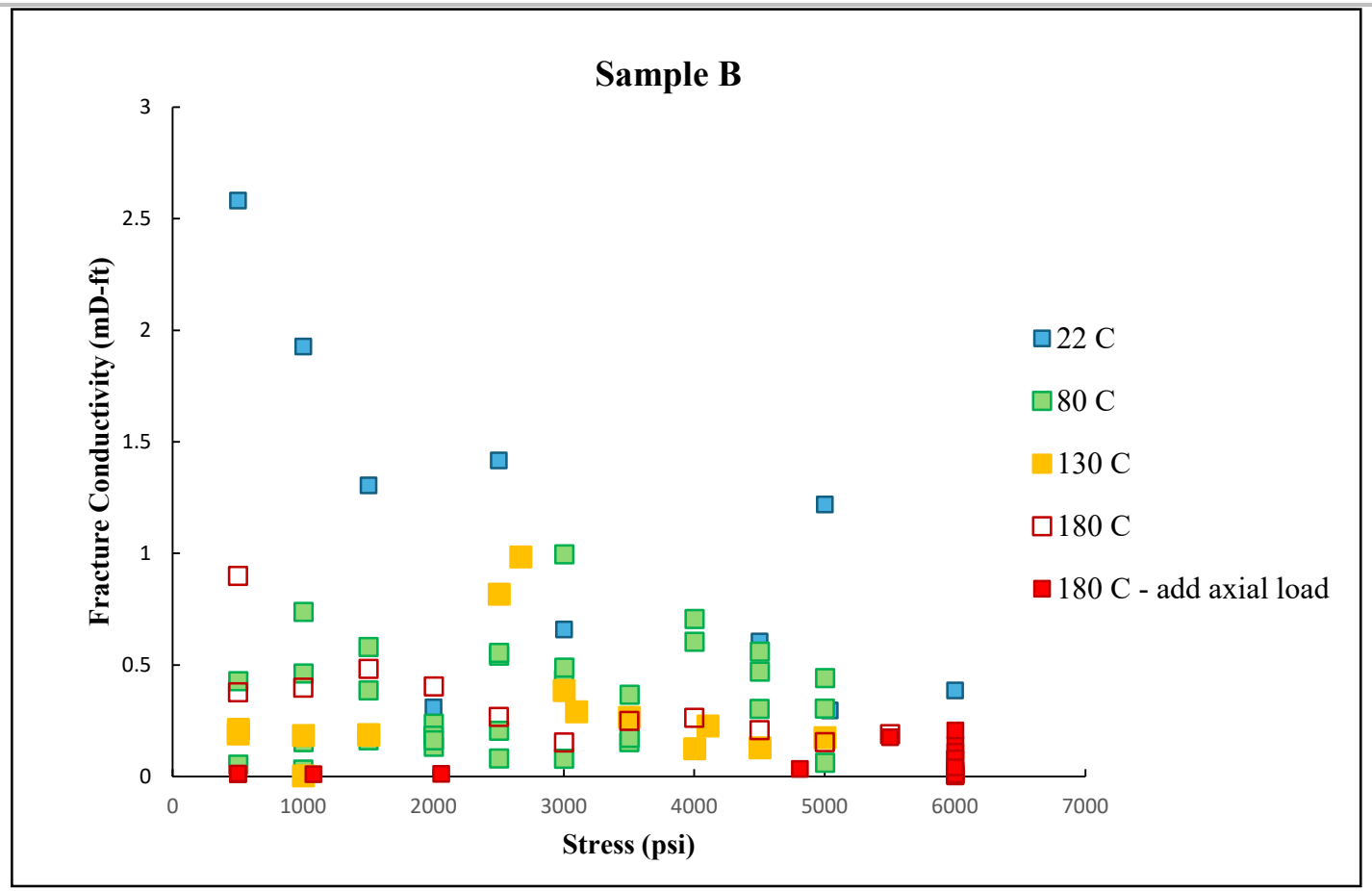

Overall, conductivity decreases with both increasing temperature and applied stress. While data shows some scattering - indicative of unstable flow behavior characteristic of proppant packs (unlike consolidated rock formations) - the decreasing trend remains statistically evident.

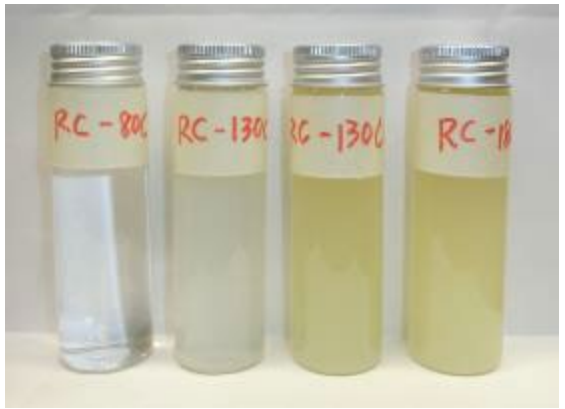

Overflow following thermal treatment at 80°C, 130°C (early time and late time), 180°C (left to right). The progressive darkening of solution color indicates increasing dissolution of material components over time and elevated temperatures.

Sample B (RC proppant)

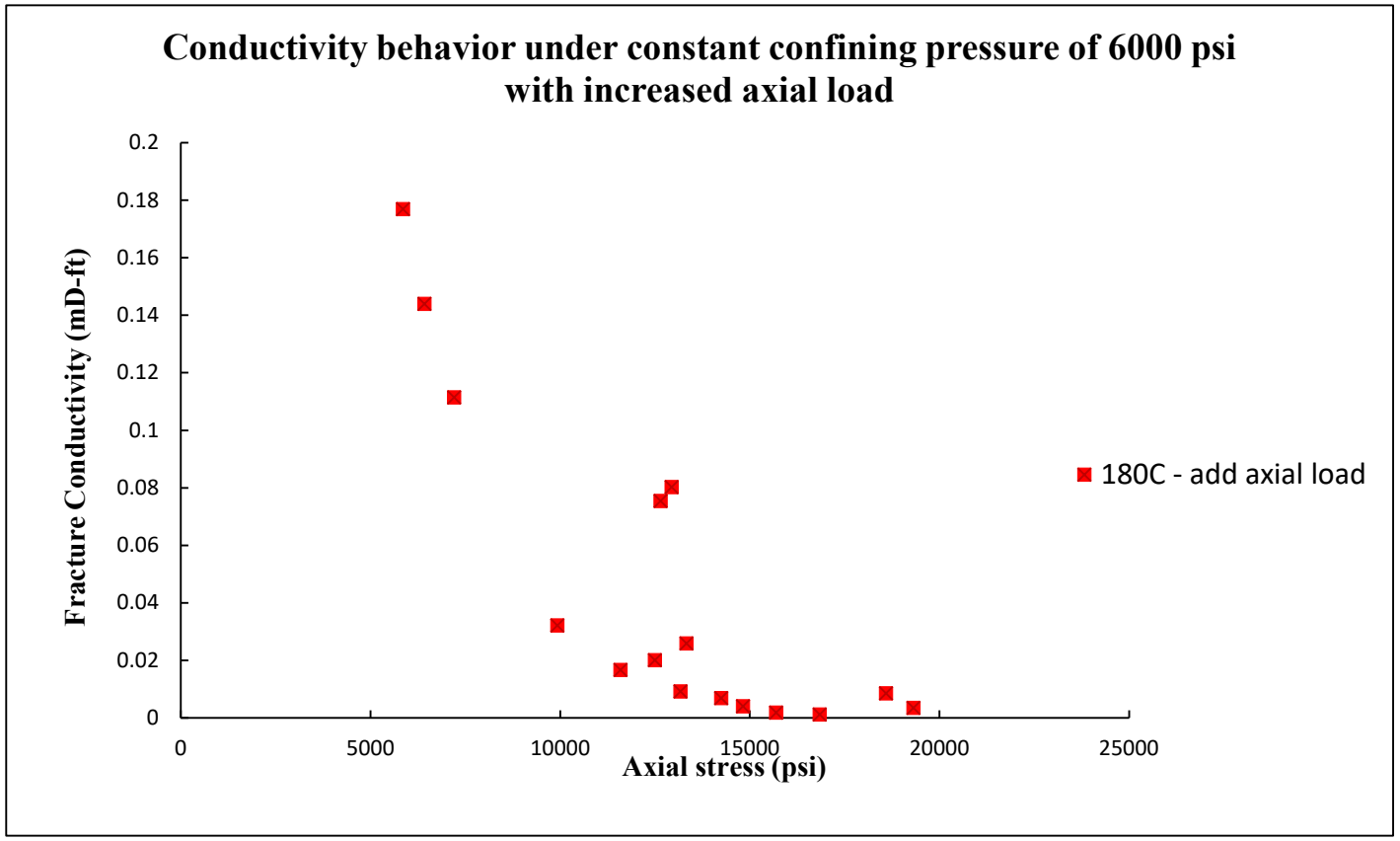

This figure presents a detailed view of the high-stress range from the previous slide. While the earlier slide illustrated conductivity behavior under hydrostatic compression, this figure shows that under a constant confining pressure of 6000 psi, increasing axial stress leads to a further decrease in conductivity.

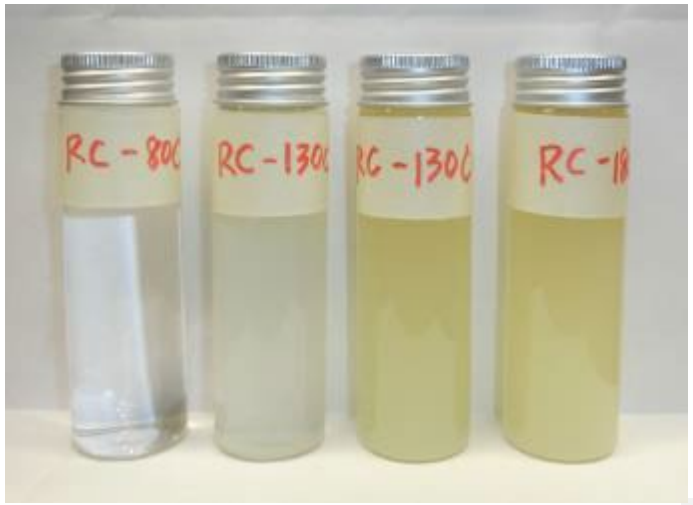

Sample ReB (RC proppant)

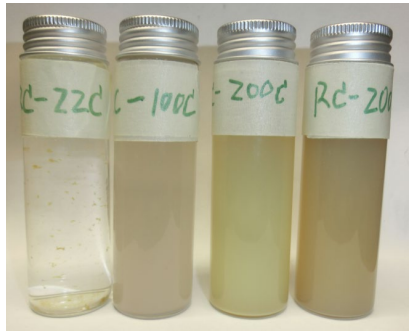

Overflow collected after heating at 100°C and 200°C (first and second day). Over time, more material appears to dissolve, as indicated by the progressively darkened color of the fluid.

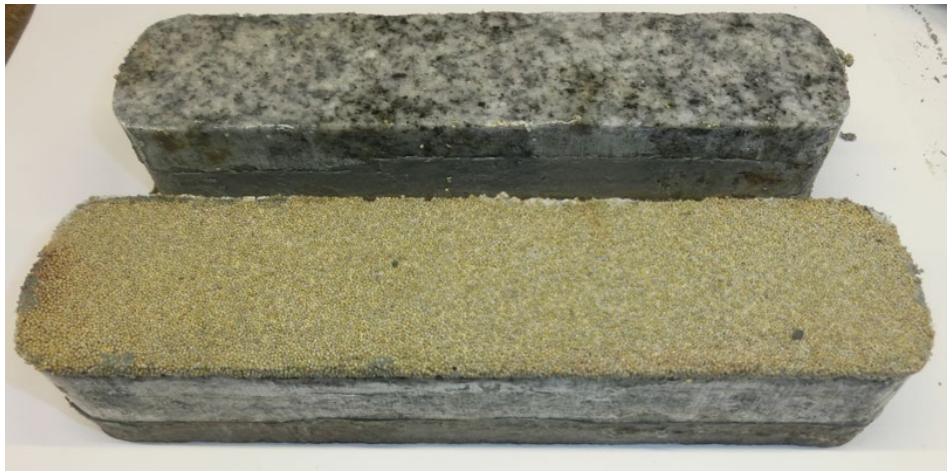

Proppant bed after exposure to high temperature and pressure. The bed remains largely intact, indicating strong structural stability under simulated downhole conditions.

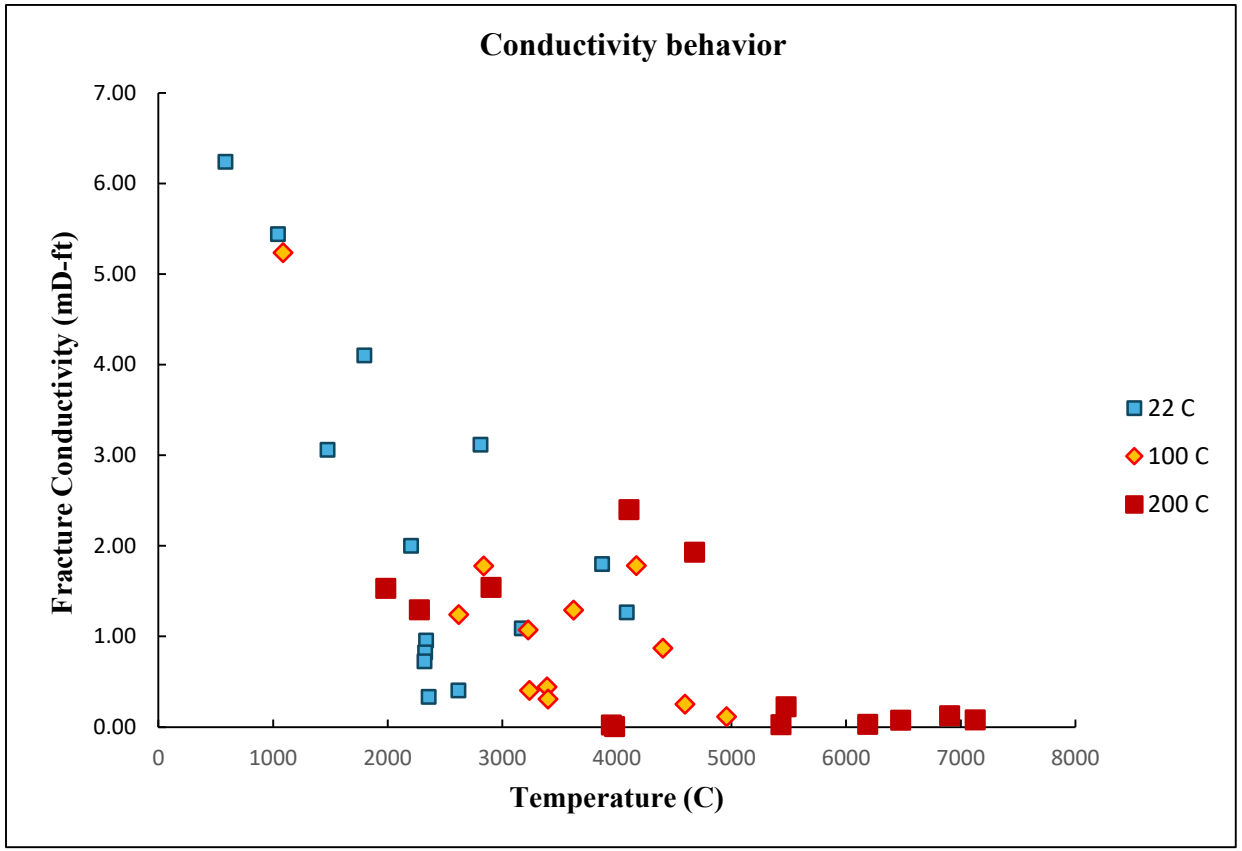

Fracture conductivity behavior during heating and stress cycling. Overall, conductivity decreases with increasing temperature and applied stress. While some fluctuations are observed, the general trend remains clear, indicating a progressive reduction in flow capacity under coupled thermal and mechanical loading.

Sample C (PC proppant)

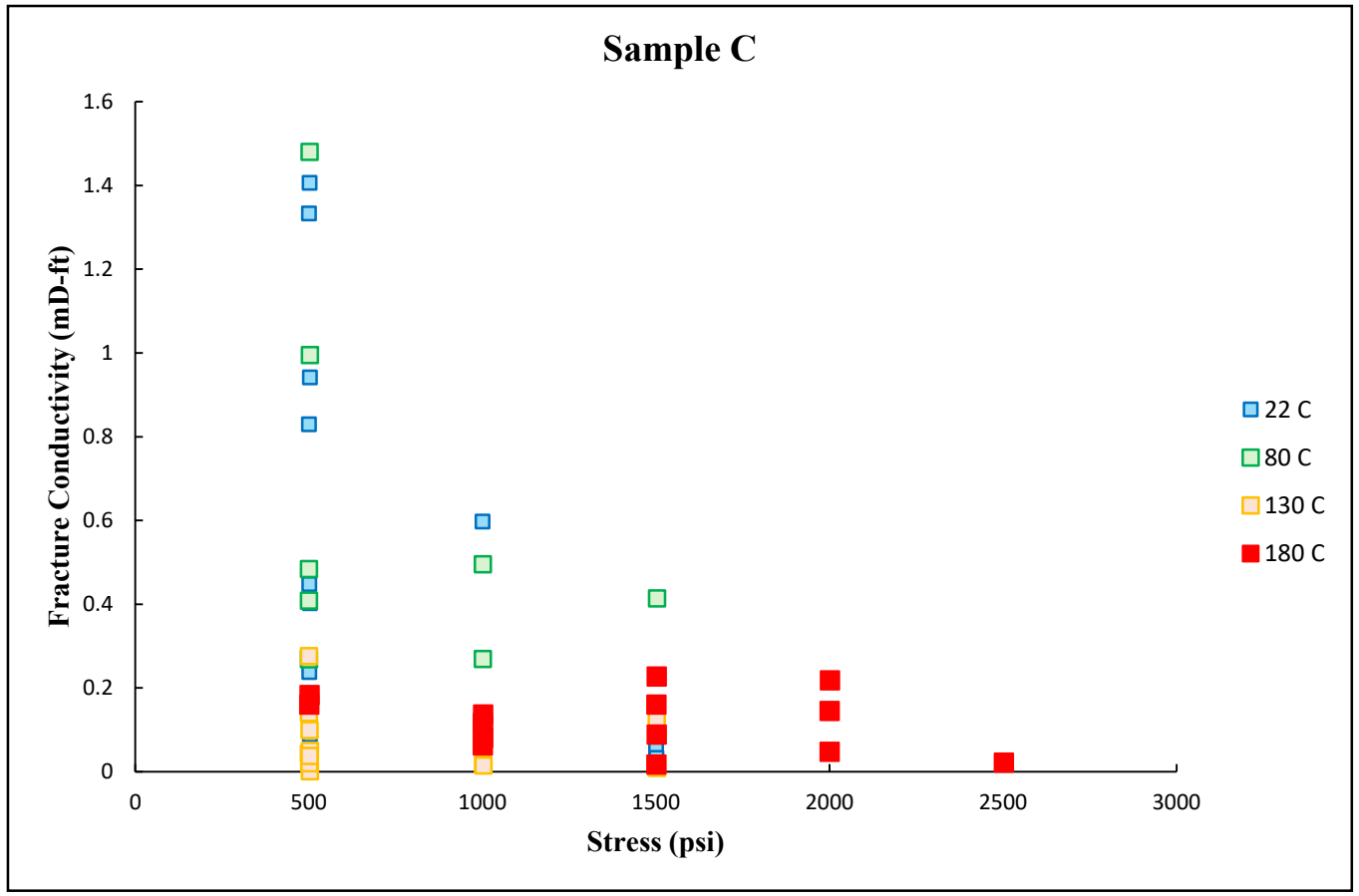

Overall, fracture conductivity decreases with both increasing temperature and applied stress. At lower temperatures (22°C and 80°C), conductivity is more sensitive to stress changes, while at 180°C, it remains low even under low stress—indicating possible irreversible thermal effects on proppant structure.

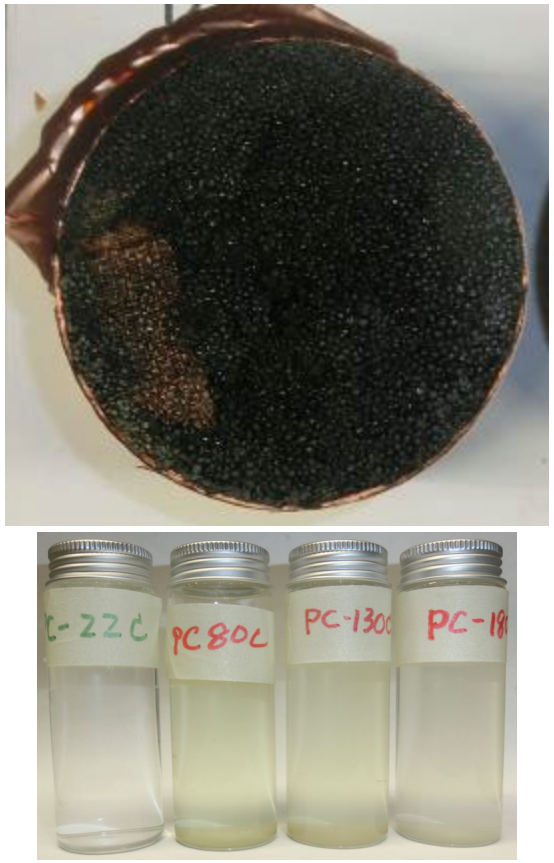

Overflow following thermal treatment at 80°C, 130°C 180°C (left to right). The overflow does not exhibit progressive darkening with increasing temperature. Some color fading was observed at 80°C, likely due to surface washing rather than chemical alteration. (*need further verification*)

Test results – Summary

Sample ID	Proppant type	Proppant bed shape	Delta P range (psi)	Flowrate range (ml/min)	Conductivity range
Sample A	LDC	circular	0.50~20.0	0.001~5.0	Drops from 20 md-ft or above at room temperature to that below 1e-3 at 180 ºC
Sample ReA	LDC	rectangular	0.35~10.0	0.001~10.0	Drops from 20 md-ft or above at room temperature to that below 1e-2 at 220 ºC
Sample B	RC	circular	0.15~17.5	0.001~5.0	Drops from 10 md-ft or above at room temperature to that below 1e-2 at 180 ºC
Sample ReB	RC	rectangular	0.70~20.0	0.001~10.0	Drops from 10 md-ft or above at room temperature to that close to 1e-2 at 200 ºC
Sample C	PC	circular	0.20~10.0	0.001~5.0	Drops from 5 md-ft or above at room temperature to that close to 1e-2 at 180 ºC

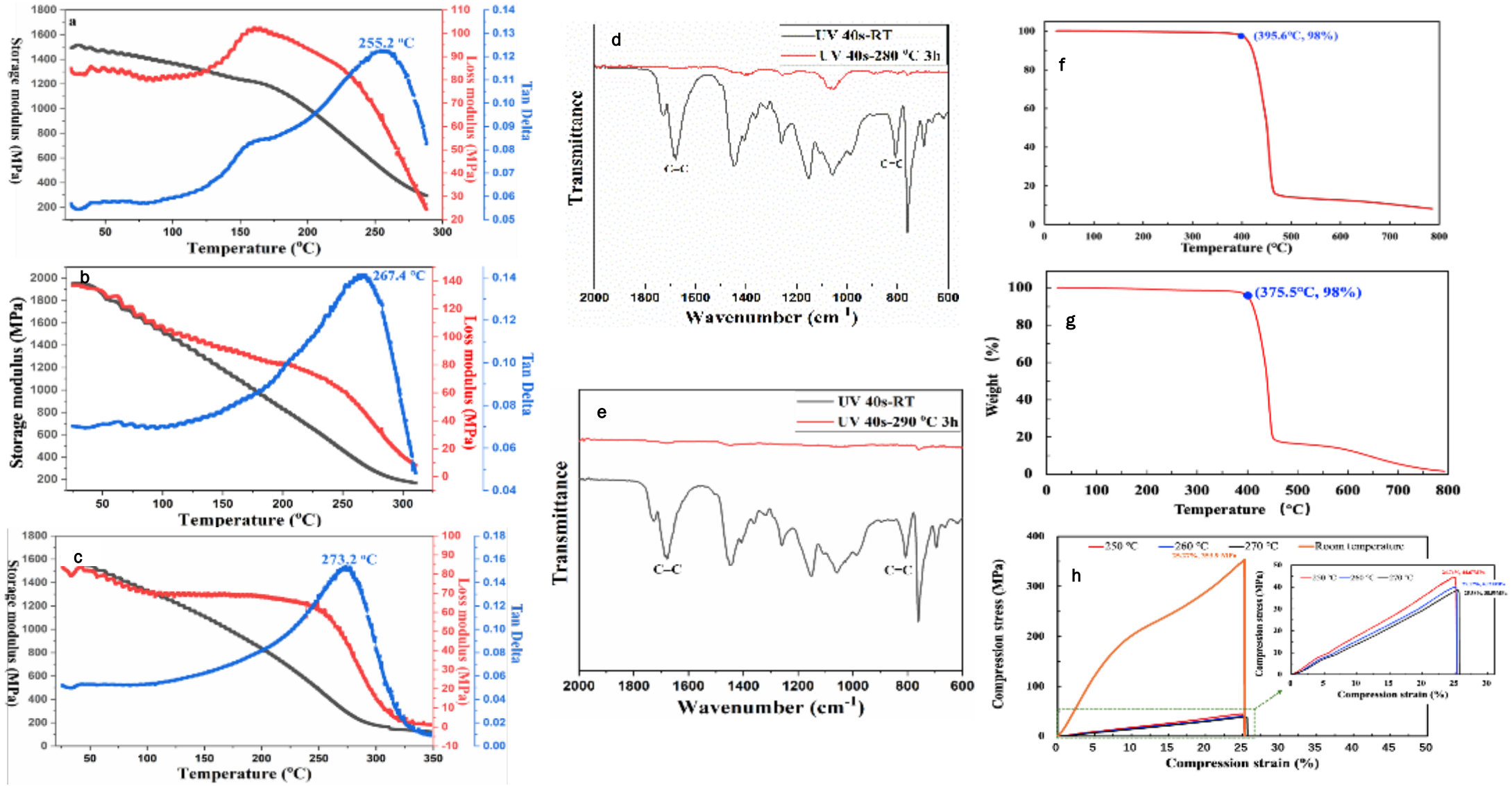

(a) DMA test results of the HTTP post-cured at 280 °C for 3 hours. (b) DMA test results of the HTTP post-cured at 290 °C for 3 hours. (c) DMA test results of the HTTP post-cured at 310 °C for 3 hours. (d) FTIR characterization of the HTTP post-cured at 280 °C for 3 hours. (e) FTIR characterization of the HTTP post-cured at 290 °C for 3 hours. (f) TGA test results of the HTTP post-cured at 280 °C for 3 hours. (g) TGA test results of the HTTP post-cured at 290 °C for 3 hours. (h) Uniaxial compressive stress-strain test results of the HTTP post-cured at 290 °C for 3 hours. The compression test was conducted at 250 °C, 260 °C, and 270 °C, respectively.

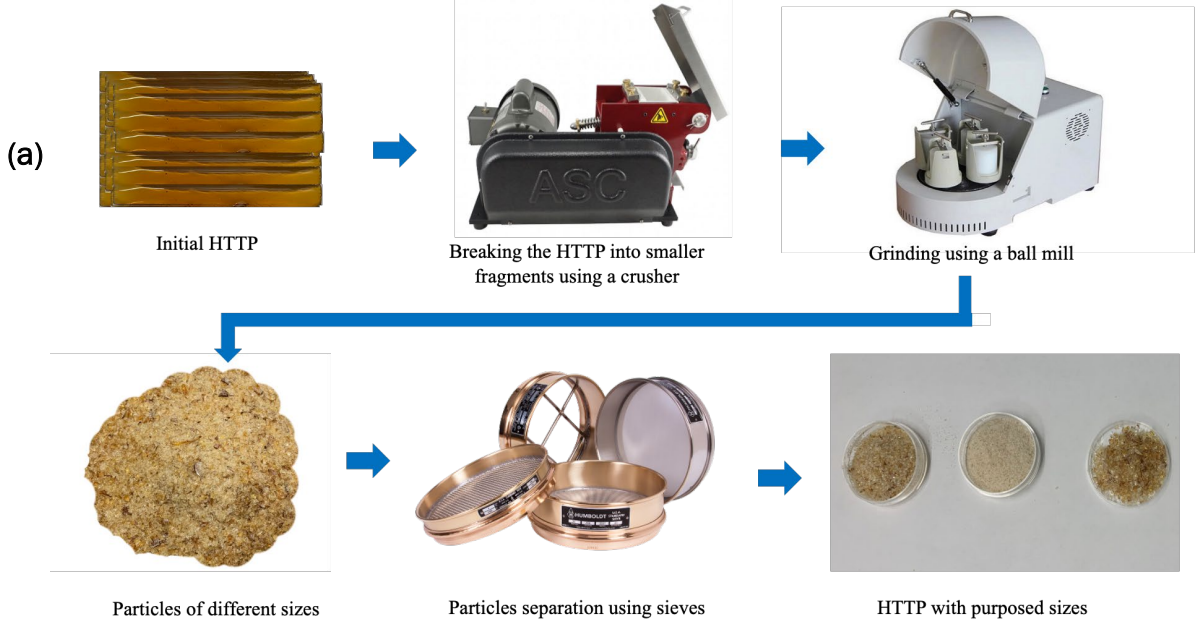

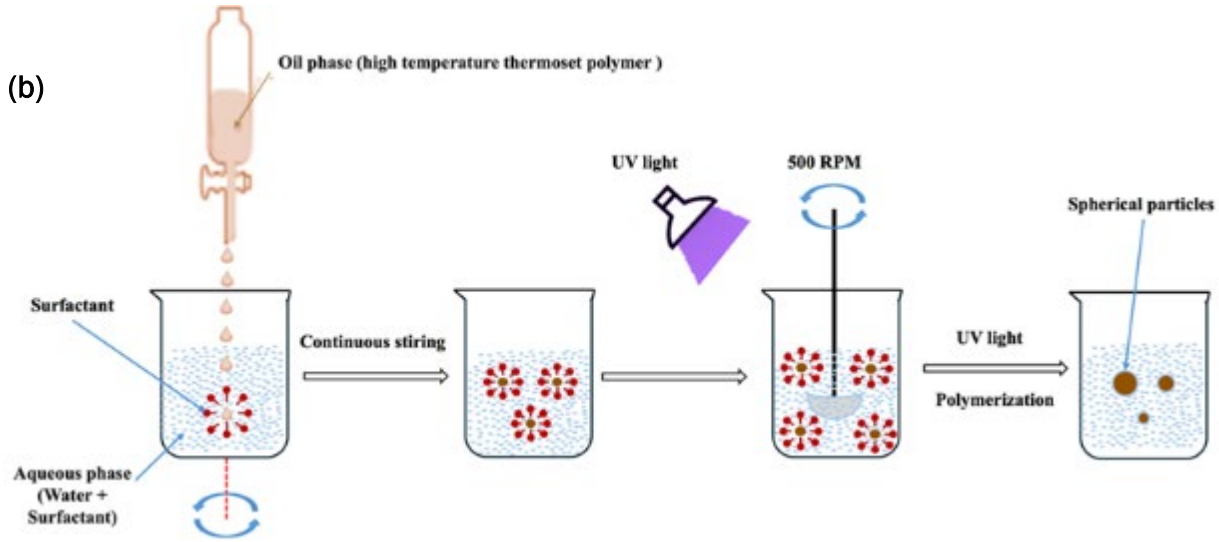

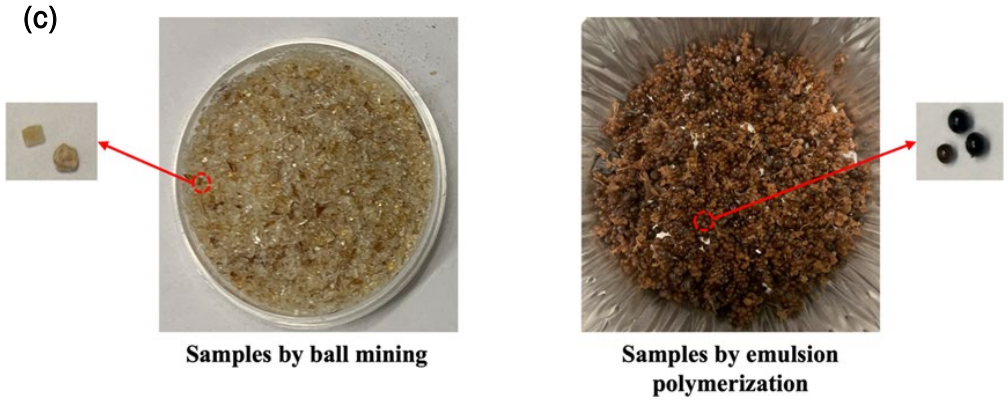

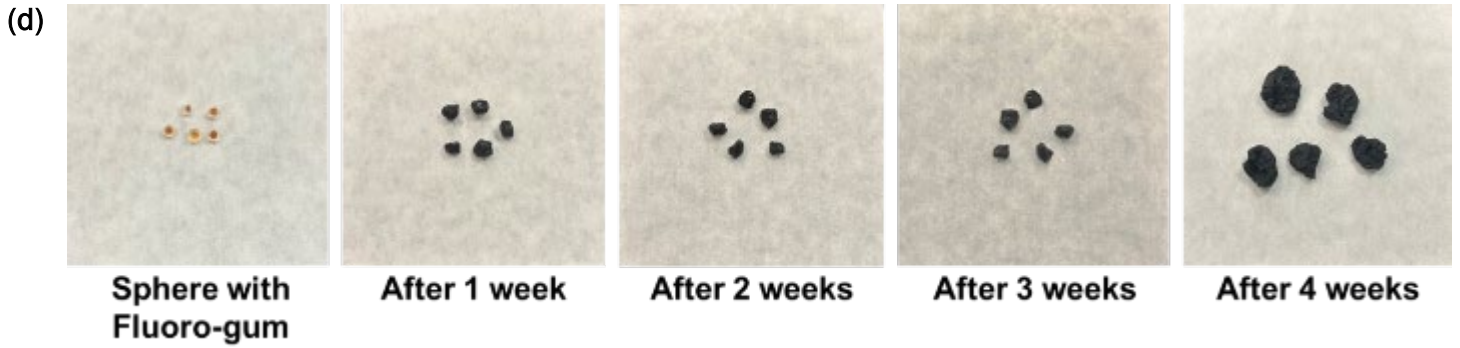

(a) Procedures to convert HTTP bulk to particles through ball milling. (b) Procedures to produce HTTP particles directly using emulsion polymerization. (c) The prepared HTTP particles as proppants. (d) The HTTP particles were immersed in superhot water (200 oC) for different time periods (original, 1 week, 2 weeks, 3 weeks, and 4 weeks). The HTTP particles were coated by a crosslinked fluorinated rubber layer. It is seen that the rubber coating layer darkened and swelled overtime.

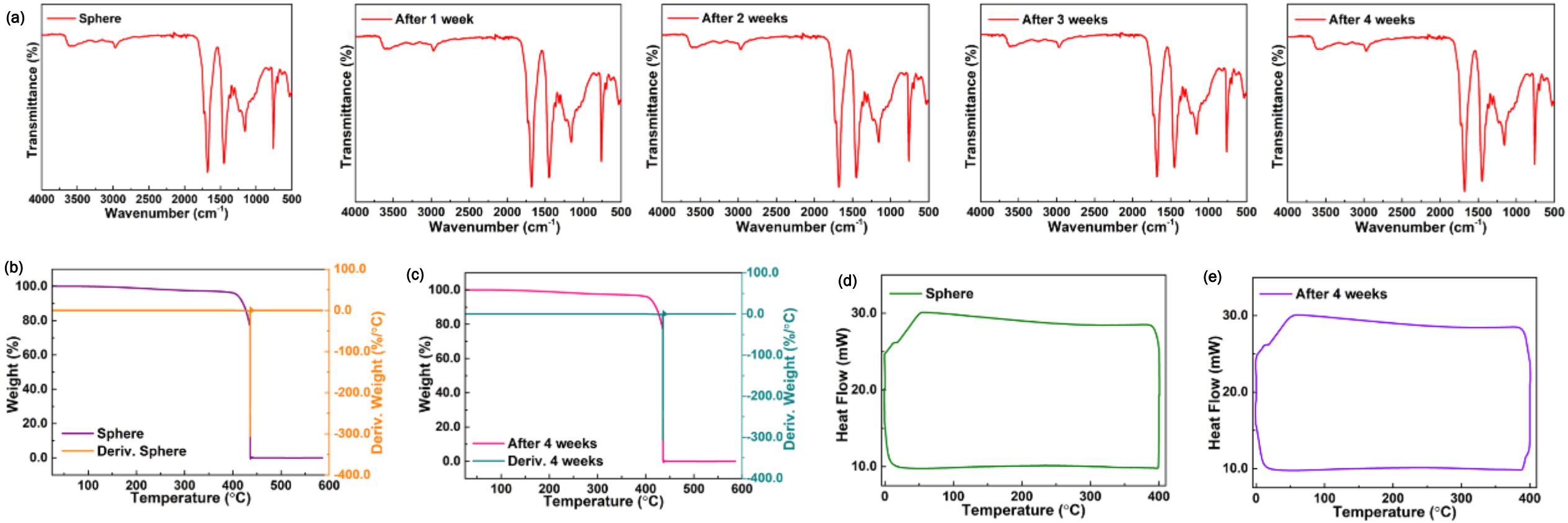

(a) FTIR characterization of the fluorinated rubber coated HTTP particles after immersing in 200 °C water for 1 week, 2 weeks, 3 weeks, and 4 weeks. The test results show that the polymer is chemically stable. However, we saw the change in surface color and swelling of the coating rubber layer. We will continue to improve the coating layer. (b) TGA test results of the original HTTP particles. (c) TGA test results of the fluorinated rubber coated HTTP particles after immersing them in 200 °C water for 4 weeks. (d) DSC test results of the original HTTP particles. (e) DSC test results of the fluorinated rubber coated HTTP particles after immersing them in 200 °C water for 4 weeks.

Modeling PSD Effects: Results

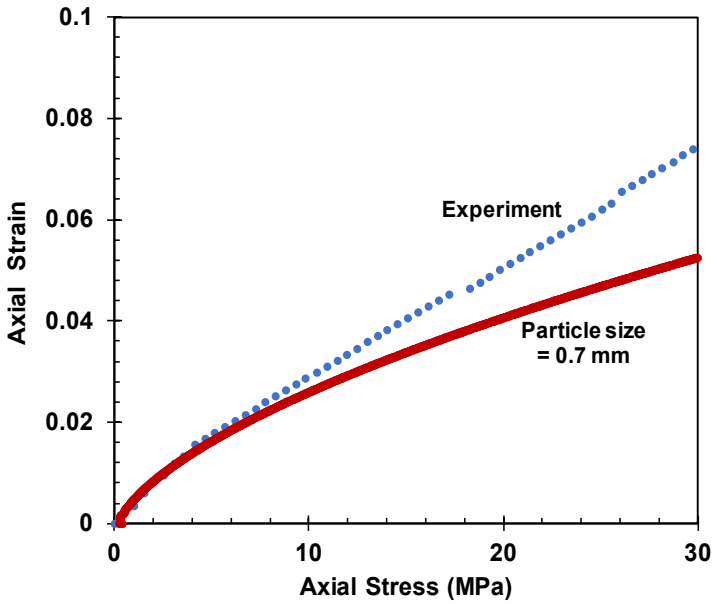

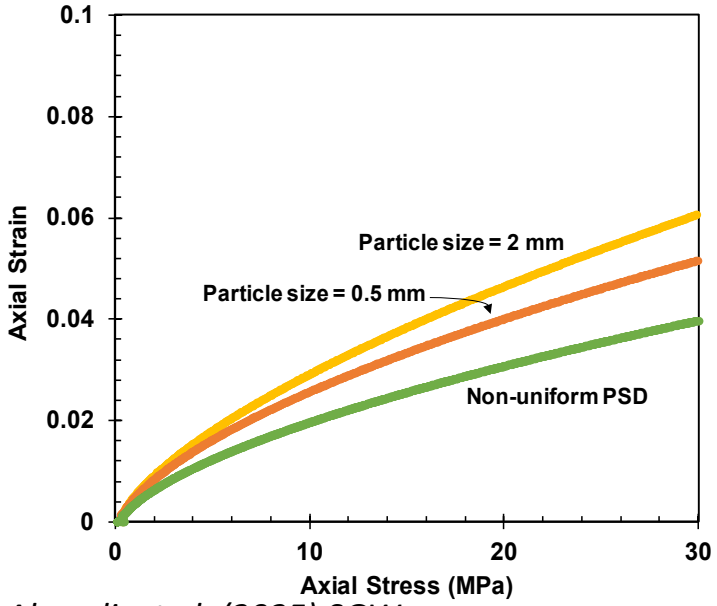

Alasadi, et al. (2025) SGW

40x LDC

D_p = 0.7 mm

Kozeny-Carman

$$K = \frac{1}{C_{C-K}} \frac{1}{S_0^2} \frac{e^3}{1+e}$$

Parameter (Unit)	Value
Packing pressure, P_m (MPa)	4.0
Friction coefficient during packing, μ_{CA}	0.2
Damping coefficient, α	0.7
Axial deformation rate, δ_v (mm/s)	200
Pack diameter, D (mm)	75
Pack height, H (mm)	25
Young's Modulus, E (GPa)	32
Friction coefficient, μ	0.5
Poisson's ratio, ν	0.2

Uniform PSD force chains

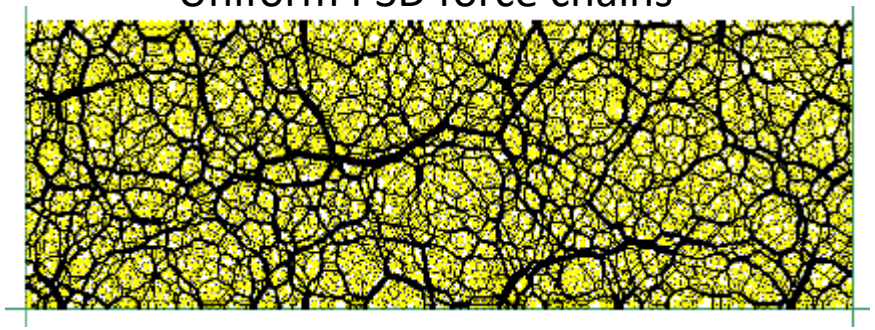

Non-uniform PSD force chains

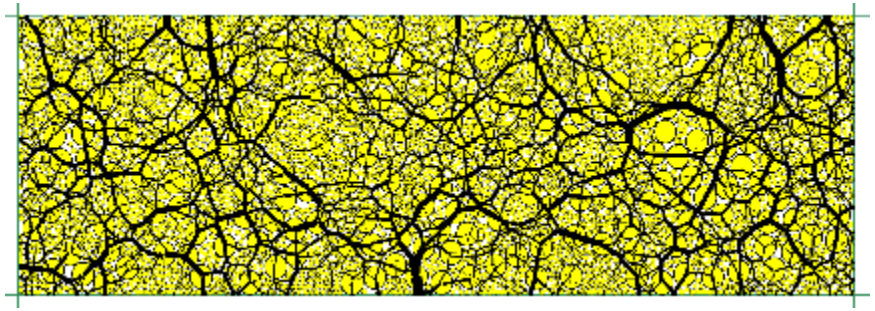

Size (mm)	K_i (D)	↓ %
0.5	0.026	40.3
0.7	0.052	39.2
2.0	0.430	37.5
50% 0.5 & 50% 2	0.026	48.2

Small particles fill the voids, blocking the flow paths.
Packs of large particles with uniform PSD have the highest initial K and lowest K reduction but are more prone to crushing.

Modeling Particle Shape Effects: Numerical Model Setups

Selected and Fabricated Particle Shapes

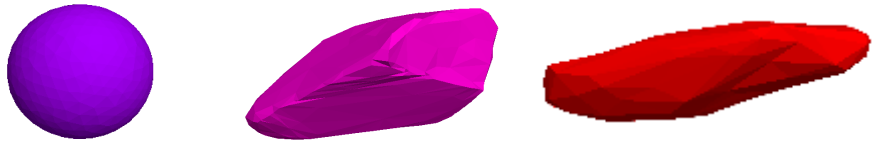

Spherical (S)
AR = 1:1:1

Angular (A)
AR = 2:1:1

Elongated (E)
AR = 3:1:1

3D-printed PLA Spherical Particles

Particle-particle:
Hertzian contact
Particle-wall:
Linear contact

Oedometer Test (ODT)

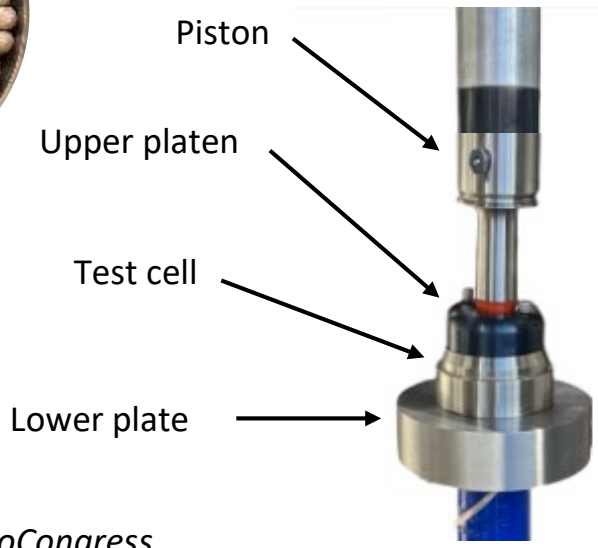

Parameters	Values
Nominal particle size (mm)	5
Particle density, ρ_p (g/cc)	1.3
Local damping coefficient, α	0.7
Viscous damping coefficient, α_h	0.5
Hertzian Contact Model Parameters:	
Young's Modulus, E_p (GPa)	1.9
Poisson's ratio, v_p	0.33
Interparticle friction coefficient, μ_p	0.5
Linear Contact Model Parameters:	
Wall normal stiffness, k_{nw} (MPa)	1
Wall shear stiffness, k_{sw} (MPa)	1
Wall friction coefficient, μ_w	0

3D ODT Setup

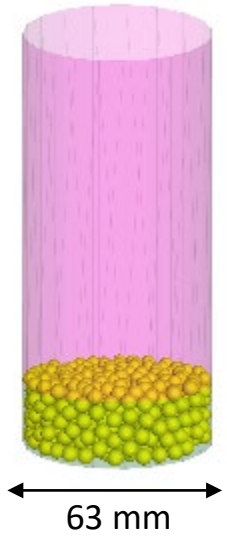

3D DST Setup

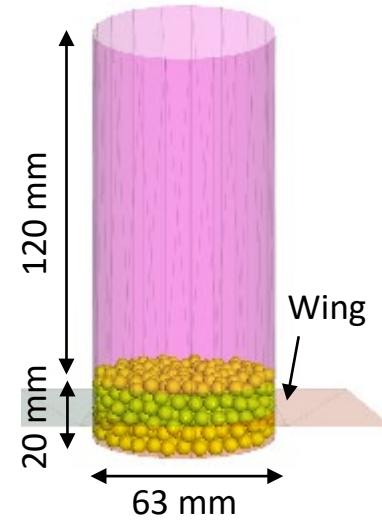

Direct Shear Test (DST)

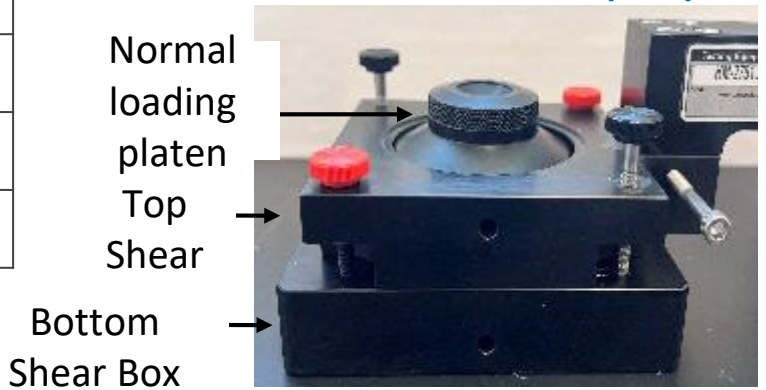

Modeling Particle Shape Effects: Results

PLA ODT Model Results

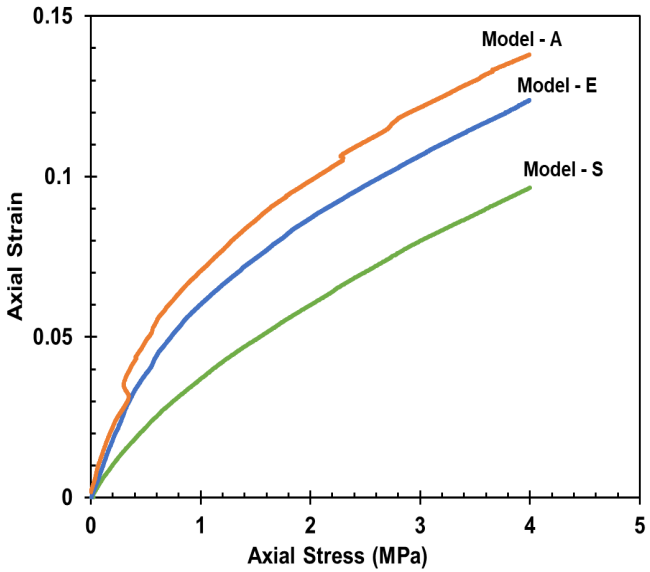

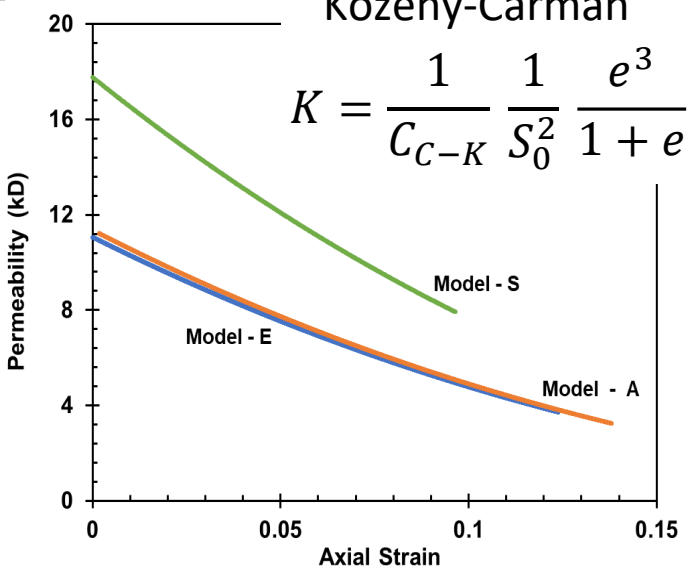

Kozeny-Carman

$$K = \frac{1}{C_{C-K}} \frac{1}{S_0^2} \frac{e^3}{1+e}$$

Spherical particles show a stiffer response than non-spherical particles.
Spherical particles show steeper permeability reduction with axial strain due to the smaller surface area per unit volume.

Spherical particles show lower shear strength as their rolling limits interlocking and weakens force chains.

PLA DST Model Results

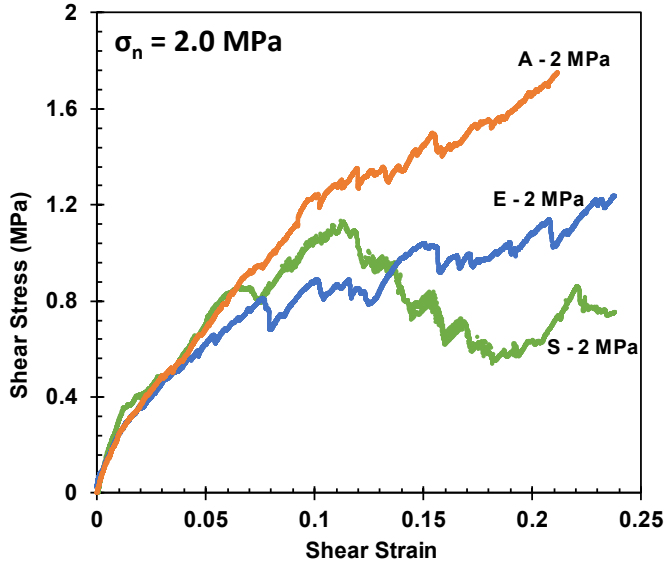

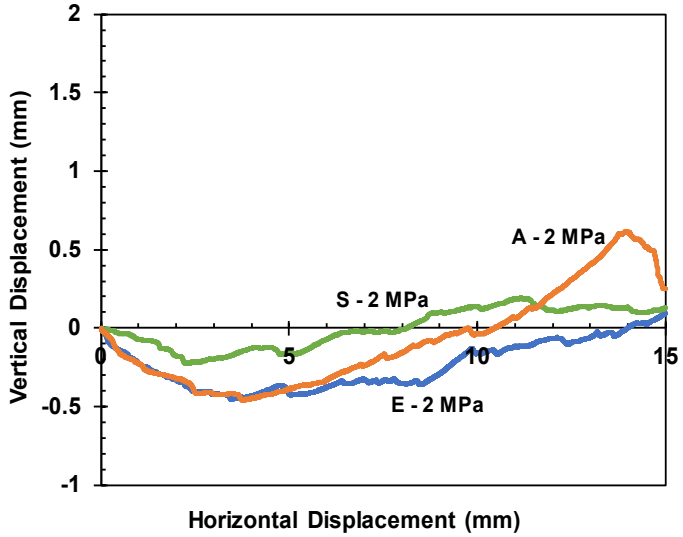

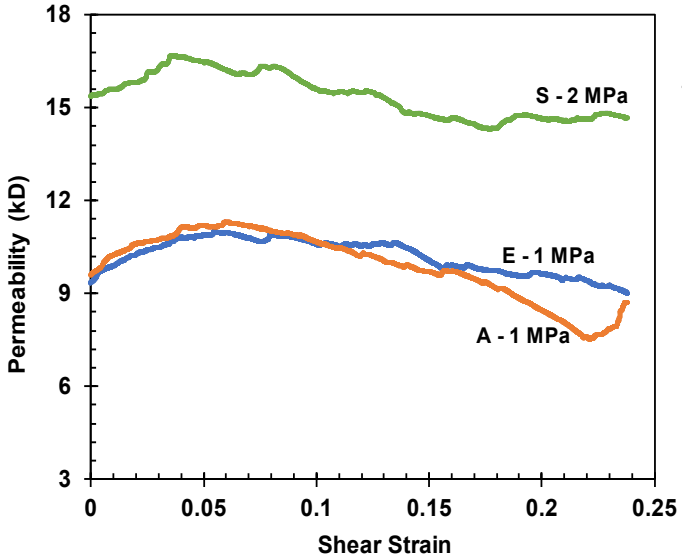

The pack of spherical particles remains the most permeable during shear as it dilates with particles rolling and sliding past each other.

Alasadi, et al. (2026) GeoCongress

Technical Accomplishments

Milestone Table

9-3664 OU PI: Ahmad Ghassemi

X Original Contractual Due Date
O Active R&D
O Adjusted Milestone Due Date
● Final (Completed)
D Deliverable (Report required)

	Budget Year	Year 1				Year 2				Year 3			
	Actual Qtr.	Q2 24	Q3 24	Q4 24	Q1 25	Q2 25	Q3 25	Q4 25	Q1 26	Q2 26	Q3 26	Q4 26	Q1 27
	Project Qtr.	Q1	Q2	Q3	Q4	Q5	Q6	Q7	Q8	Q9	Q10	Q11	Q12
Project Milestones	Deliverable												
Task 0 – Project Management and Planning			●										
Task 1 – Procure proppant materials and consider modifications if necessary and determine their index properties. Examine the durability of selected proppant materials in the presence of geothermal fluids at high temperatures													
Sub Task 1.1 – Selection of the intervals for stimulation using all available relevant data from FORGE, including geological earth model, petrophysical and rock mechanical characterization, microseismic data, well logs and images, and in-situ stress estimates				X									
Milestone 1.1 -Review the selected proppant materials and determine their index properties.	D				X								
Sub Task 1.2 – Characterize the resistance of selected proppant materials to geothermal fluids and high temperatures. The resistances of proppants to geothermal fluids and high temperatures are crucial to sustaining hydraulic conductivity in geothermal reservoir stimulation.					X								
Milestone 1.2 -Characterize the resistance of selected proppant materials to geothermal fluids and high temperatures.					X								
Task 2 – Design, synthesis, and characterization of polymeric proppant													
Milestone 2.1-A new high temperature thermoset is designed, synthesized, and tested.	D						X						
Task 3 – Determination of crush resistance (K-value) and crush strength for both dry and wet-heated samples for the uncoated/untagged proppant materials; study failure mechanisms and modes using modeling and comparison with test results													
Sub Task 3.1 – Conduct ISO crush tests for both dry and wet-heated samples for the uncoated/untagged proppant materials. The crush resistance test follows the prescribed guidelines in the ISO 13503-2 standard.							X						
Milestone 3.1 -Complete the determination of crush resistance (K-value) for both dry and wet-heated samples for the uncoated/untagged proppant materials. Index properties.						X							
Sub Task 3.2 – Conduct modified ISO crush tests to determine the crush strength of both dry and wet-heated samples for the uncoated/untagged proppant materials.							X						
Milestone 3.2 -Complete the determination of crush strength for both dry and wet-heated samples for the uncoated/untagged proppant materials using the modified ISO crush testing.							X						
Sub Task 3.3 – Conduct the modified triaxial crush tests using Sierra White granite slabs for the uncoated/untagged proppant materials.								X					
Sub Task 3.4 – Quantify/map the impact of proppant size, shape, packing on strength and potential failure modes, as well as the stress-dependent hydromechanical behavior of selected materials under high-stress (35-70 MPa).								X					
Milestone 3.3 -Complete the determination of crush strength of the uncoated/untagged proppant materials through the modified triaxial crush testing. Simulations of controls on proppant and pack strength completed	D							X					
Task 4 – Determination of crush resistance (K-value) and crush strength for both dry and wet-heated samples for the uncoated/untagged proppant materials; study failure mechanisms and modes using modeling and comparison with test results													
Milestone 4.1 -Completion of long-term hydraulic conductivity under HTHP conditions for the uncoated/untagged proppants, and correlation of conductivity, closure stress, and temperature. Index properties.	D							X					
Sub Task 4.2 –Quantify/map the impact of proppant size, shape, packing on strength and potential failure modes, as well as the stress-dependent thermo-hydromechanical behavior of selected particulate materials under high-stress (35-70 MPa) and at least 250C							X						
Go/No-Go Decision Point #1: Selected and manufactured proppants characterized, crush tests and long-term conductivity tests completed (at least 2 tests per proppant type) under pressure and temperature conditions of 35-70 MPa, and up to 250C.	D				X								
Task 5 – Make tagged proppants (electromagnetic responsive proppant) and procure other coated proppants, garnet and petcoke from HERO													
Milestone 5.1 -Electromagnetic responsive polymeric proppant fabricated, characterized, and tested, others procured										X			
Task 6 – Determination of crush strength, crush resistance (K-value), and the percentage of fines generated by crushing for both dry and wet-heated samples for the coated/tagged proppant materials													
Sub Task 6.1 – Determination of long-term hydraulic conductivity of the tagged/coated proppant materials at various stress and temperature conditions (at least 2 tests per proppant type) under pressure and temperature conditions of 35-70 MPa, and up to 250C.										X			
Milestone 6.1 -Complete the determination of crush strength, crush resistance (K-value), and the percentage of fines generated by crushing for both dry and wet-heated samples for the coated/tagged proppant materials.										X			
Task 7 – Determination of long-term hydraulic conductivity of the tagged/coated proppant materials at various stress and temperature conditions (at least 2 tests per proppant type) under pressure and temperature conditions of 35-70 MPa, and up to 250C.													
Milestone 7.1 -Long-term hydraulic conductivity tests under HTHP conditions completed for the coated/tagged proppants; obtained conductivity, closure stress correlations.											X		
Go/No-Go Decision Point #2: Conductivity experiments completed, simulations illustrate expected performance in terms of transport and conductivity retention.	D								X				
Task 8 – Examine the hydraulic conductivity, placement, and electrical detectability of the coated/tagged proppant materials in large fracture(s) created in granite blocks.													
Milestone 8.1 -Determination of the hydraulic conductivity and the electrical conductivity of the coated/tagged proppant materials in large granite fracture under true-triaxial stresses. At least 2 tests completed													X
Task 9 – Quantify/map the cyclic stress- and temperature-dependent hydro-thermo- mechanical behavior of selected particulate materials under high-stress (35-70 MPa) and high-temperature (250-350 °C) conditions													
Milestone 9.1 -Illustrative scoping simulations completed, findings collated.													X
Task 10 – Summary of findings and recommendation for field trial	D												X

UTAH FORGE U.S. Department of Energy

Technological Advancement and Data Dissemination

- Sutradhor, A.S., Ghassemi, A. 2025. Hydraulic Fracture Propagation and Proppant Transport in Anisotropic Rock Formations. 59th US Rock Mechanics/Geomechanics Symposium held in Santa Fe, New Mexico, USA.
- Sutradhor, A.S., Ghassemi, A. 2025. Crush Resistance and Packing Strength of Candidate Proppant for Enhanced Geothermal Systems. PROCEEDINGS, 50th Workshop on Geothermal Reservoir Engineering Stanford University, Stanford, CA
- Liu, B., Ghassemi, A. 2024. Modeling proppant transport and settlement in 3D fracture networks in geothermal reservoirs. Geothermics.
- Alasadi, A., Potyondy, D., Ghassemi, A., and Roshankhah, S. (2025). DEM-Based Analysis to Reveal the Effects of Particle Size Distribution on Deformational Behavior of Particulate Packs, Stanford Geothermal Workshop, Palo Alto, CA, February 10-12.
- Alasadi, A., Potyondy, D., Ghassemi, A., and Roshankhah, S. (2026). Influence of Particle Shape on Deformational Behavior of Particulate Packs Using Experimental and DEM Modeling, GeoCongress, Salt Lake City, UT, March 9-12.

Mandatory- may utilize multiple slides

Future Directions

- Continue to determine crush resistance (K-value) and crush strength for both dry and wet-heated samples of new proppants
- study failure mechanisms and modes using modeling and comparison with test results (M3-M12).

- Determine long-term hydraulic conductivity of the uncoated/untagged proppant materials at various stress and temperature conditions, smooth and rough fracture

Examine the hydraulic conductivity, and electrical detectability of the coated/tagged proppant materials in large fracture(s) created in granite blocks. (M24- 30)

Quantify/map the cyclic stress- and temperature-dependent hydro-thermo-mechanical behavior of selected materials under HTHP conditions. Simulate proppant transport, placement and proppant bed formation using different proppants and fluid with temperature dependent viscosity (M24-30).

Mandatory- may utilize multiple slides

Summary

- **Conductivity Degradation Trends**

Conductivity generally decreases with increasing axial stress / confining pressure and temperature. Irreversible reductions suggest that the proppant bed undergoes permanent deformation or rearrangement under thermal-mechanical loading.

- **Thermal Stability and Chemical Integrity**

Proppants exhibit different levels of thermal and chemical stability when exposed to elevated temperatures over time. Typically, the overflow water becomes progressively darker with continued heating, suggesting that certain components within the proppants are dissolving or chemically degrading. This visual indicator reflects the ongoing interaction between the proppant material and the surrounding fluid under high-temperature conditions.

- **Impact of Loading History**

The conductivity behavior of proppant beds is not only dependent on the current stress state but also strongly influenced by the stress path or loading history. These path-dependent effects highlight the importance of understanding the mechanical memory of proppants and their capacity to sustain conductivity under cyclic or fluctuating stress conditions, which are often encountered in subsurface environments.

THANK YOU

Funding provided by DOE EERE Geothermal Technologies Office to Utah FORGE and the University of Utah under Project DE-EE0007080 Enhanced Geothermal System Concept Testing and Development at the Milford City, Utah Frontier Observatory for Research in Geothermal Energy (Utah FORGE) site with additional support from Utah Trust Lands Administration, Beaver County, the Governor's Office of Energy Development, and Smithfield Foods.

UTAH FORGE U.S. Department of Energy